

Temperature-dependent work functions of free alkali-metal nanoparticles

Kin Wong, George Tikhonov,* and Vitaly V. Kresin

Department of Physics and Astronomy, University of Southern California, Los Angeles, California 90089-0484

(Received 22 April 2002; published 4 September 2002)

Photoionization yields have been measured as a function of temperature for the alkali metals Li, Na, and K in the form of free nanometer-sized clusters in a beam. The data can be fitted very well by a finite-temperature Fowler plot, originally derived for bulk surfaces. The resulting temperature-dependent ionization thresholds match precisely the literature work function values and are, within the experimental uncertainties, in agreement with recent theoretical models for thermal shifts of the work function.

DOI: 10.1103/PhysRevB.66.125401

PACS number(s): 79.60.-i, 73.30.+y, 36.40.Vz

I. INTRODUCTION

Most introductory discussions of the photoelectric effect of metals do not pay much attention to possible variation of the surface work function with temperature.^{1,2} However, a large number of tabulated work functions derive from measurements at room temperature or much higher.³ The common neglect of temperature effects is justified by the fact that they are quite small, since for most metals the Fermi temperature greatly exceeds the ambient temperature. Furthermore, it is not trivial to resolve such a shift, because both the experimental precision and *ab initio* capability are typically more coarse than the effect in question.⁴⁻⁷ Nevertheless, the temperature shift of the metal work function is an interesting subject because it concerns the interplay between structural (e.g., phonon excitation, thermal expansion, melting) and electronic degrees of freedom, the behavior of surface potentials, etc. Furthermore, semiempirical theories⁷⁻¹⁰ incorporating thermal expansion effects have made specific predictions about the magnitude of the effect in various metals. Accurate measurements of work functions as a function of temperature are therefore quite instructive.

At the same time, such measurements are difficult because they impose very strict requirements on the quality and purity of the surface. For example, contamination, which itself is temperature dependent, can mask the effect completely.⁶ The situation is especially challenging with the highly reactive alkali metals.¹¹

It has been demonstrated that accurate measurements of metal work functions can be obtained by studying free nanoparticles rather than bulk surfaces.¹²⁻¹⁴ In our setup a beam of nanoscale clusters (several nm in diameter) is generated in a metal vapor condensation source; the particles are ionized by near-UV light of variable frequency, and the resulting yield of positive ions is measured. This method takes advantage of the fact that the particle flight time in a molecular beam is very short (milliseconds), and therefore surface contamination can be reduced to a minimum without a need to resort to ultrahigh-vacuum surface preparation techniques. At the same time, the use of ion-counting detection ensures high sensitivity.

We have shown previously¹⁴ that with appropriate threshold fitting, photoionization spectra of cold alkali give results which are in excellent agreement with the literature values of polycrystalline work functions. In this paper we use a modi-

fied particle source with a temperature-controlled nozzle to measure the temperature dependence of the work function for Li, Na, and K.

II. EXPERIMENTAL METHOD

The experiment is performed with a cluster beam apparatus described in detail earlier.¹⁴ Large clusters of lithium, sodium, or potassium are produced by evaporating metal from a crucible and quenching the vapor in a flow of cold helium gas. Nanoclusters condense in the aggregation zone,¹⁵ exit the source through a long nozzle (length 25 mm, inner diameter 2–3.5 mm), and form a collimated beam in free flight towards the detector. In order to control their temperature, a cylindrical thermalization tube is added to the setup as shown in Fig. 1. The tube, which is 17 cm long with an inner diameter of 11 mm, attaches directly behind the nozzle. The temperature of the tube is controlled by electrical heater coils and monitored by three thermocouples, ensuring uniform temperature distribution along the tube. It can be maintained at any temperature between 300 K and 500 K with a less than 2 K temperature difference between the ends. The geometry of the tube is chosen to obtain thermal equilibrium between the tube and the clusters. Similar constructions have been used by other groups^{16,17} and were found to be adequate to control the internal temperature of the clusters. For low-temperature measurements the heated tube is removed, in which case the clusters retain approximately the temperature of the liquid-nitrogen-cooled nozzle.

Since the particles are heavy, they are not size selected; the measurement is done on a relatively broad distribution. A linear Wiley-McLaren time-of-flight (TOF) mass spectrometer was used for an overall characterization of the nanocluster population. It also served to guard against the possibility of strong changes in the particle size distribution in response to varying source conditions. The TOF spectra indicate a distribution with an average radius of $\sim 3-5$ nm ($\sim 2 \times 10^3 - 3 \times 10^4$ atoms) and a full width at half maximum of ~ 2 nm.¹⁸ This average size is consistent with an earlier independent measurement based on electron attachment cross sections.²¹ The measured size distributions did not change upon removal of the heat tube; nor did it change when the temperature of the heat tube was varied. This indicates that the clustering process is already complete when particles exit

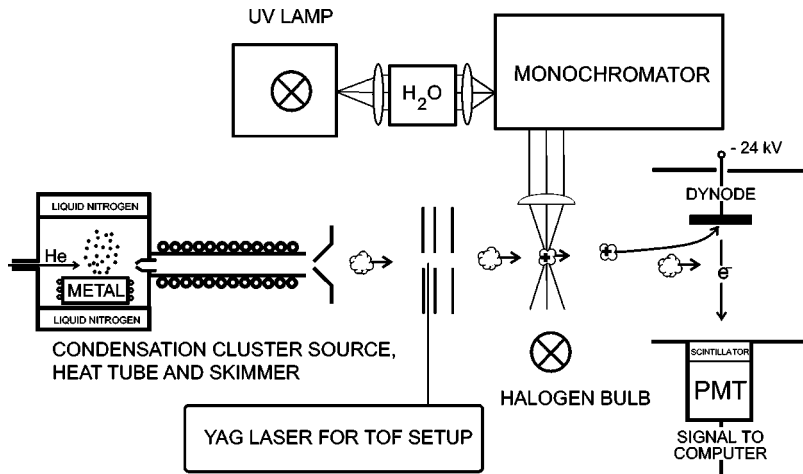


FIG. 1. Outline of the experimental setup (not to scale). The free flight distance between the skimmer and the ionization region is ≈ 2 m. Nanoparticles are formed in a vapor condensation source and pass through a thermalization tube. Monochromatic light ionizes the particles, and the ion yield is monitored by a positive-ion detector. The overall size distribution is monitored with a collinear time-of-flight setup which employs the tripled output (355 nm) of a Nd:YAG laser.

the nozzle, as expected for subsonic quench-aggregation sources.

Once the clusters leave the heating tube, they undergo a 2-m-long free flight before being ionized by monochromatic light and subsequently detected by a Daly dynode-photomultiplier ion-counting arrangement.^{22,23} The monochromatic light is generated by a regulated 1-kW Hg-Xe arc lamp. The lamp output passes through a distilled water filter, then through a monochromator which is adjusted to a band-pass of 5 nm, and is finally focused onto the cluster beam by a quartz lens. Only single-photon absorption is relevant under the present conditions. The ionizing light is chopped at 147 Hz. The cluster ion signal is recorded by a multichannel scaler which is synchronized with the light chopper.

The yield of positive ions is normalized to both the photon and nanocluster intensities. Photon intensities are measured by a silicon photodiode which can be moved *in situ* into the photon-cluster interaction region. Three photodiodes with different manufacturers' sensitivity curves were tested against each other and found to be in good agreement over the wavelength range of 350–600 nm. Cluster beam intensities were monitored by periodically recording the ion counting rate while illuminating the beam by a broadband 100-W halogen light bulb.²⁴

The ion (or, equivalently, photoelectron) yield curves were measured as a function of energy for several selected temperatures. Some representative curves are shown in Fig. 2. In the next section, we discuss the procedure of determining the ionization threshold from the data.

III. THRESHOLD BEHAVIOR

There have been only a few studies on the photoionization behavior of free nanometer-scale particles,^{12–14,25,26} and (as in the case of smaller clusters) there is no consensus on the most appropriate method of determining the ionization threshold. The problem arises from the lack of a general theory of cluster photoionization and is compounded by thermal smearing of the threshold region. As a result, a variety of more or less *ad hoc* approaches have been used in the field, including linear or exponential extrapolations and error function fits (see the references in Ref. 14). Unfortunately, the value of the ionization potential and its extrapolation to the

bulk can be significantly affected by the choice of the fitting function.¹³

A study of silver nanoparticle aerosols in gas suspension²⁷ showed that the photoion yield Y was well described by the so-called Fowler law^{6,28} for cold bulk surfaces:

$$Y \propto (h\nu - \phi_0)^2. \quad (1)$$

Here ϕ_0 is the work function and $h\nu$ is the photon energy. This is derived by evaluating the flux of those photoexcited conduction electrons whose kinetic energy of motion perpendicular to the surface exceeds the work function threshold. Surface curvature effects in large particles were found not to be significant near threshold.²⁹ Subsequently, the particle-aerosol spectroscopy was extended to some other coinage metals;¹² recently, we found that Eq. (1) also gives an excellent fit to the behavior of cold alkali nanoclusters.¹⁴

Since our focus here is on the temperature dependence of the photoelectric threshold, it is now necessary to make use of the full Fowler expression valid at finite temperatures.

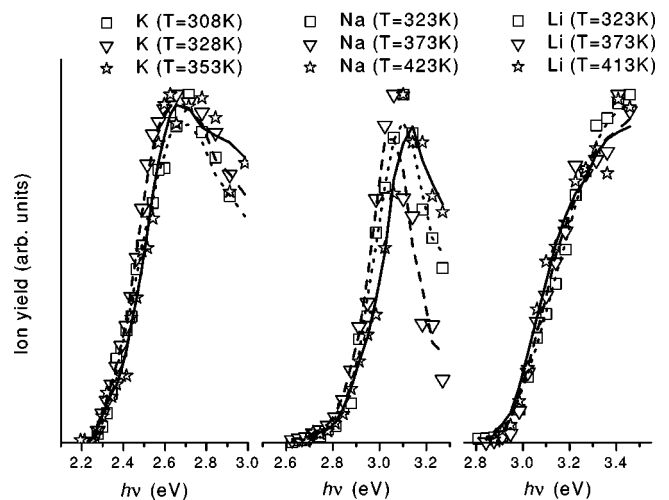


FIG. 2. Nanocluster ion yield as a function of photon energy for Li, Na, and K at selected temperatures. The lines are smoothing fits to guide the eye. Solid, dashed, and dotted lines represent the high-, intermediate-, and low-temperature data, respectively.

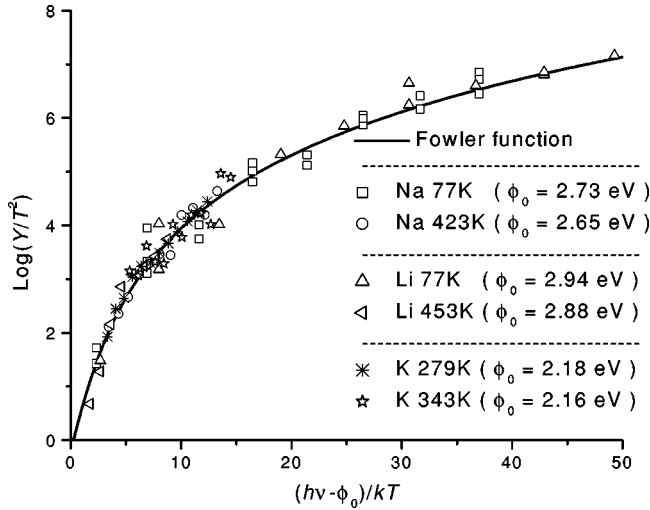


FIG. 3. Fowler plots for several selected yield curves. By varying ϕ_0 to align the data with the universal Fowler function f , the work function can be determined for various temperatures (see text for details).

When thermal smearing of the Fermi-Dirac distribution is accounted for, the equation for the photoelectron yield generalizes to

$$\ln\left(\frac{Y}{T^2}\right) = B + \ln f\left(\frac{h\nu - \phi_0}{k_B T}\right), \quad (2)$$

where f is a known function.^{6,28}

A plot of $\ln(Y/T^2)$ vs $(h\nu - \phi_0)/k_B T$ is known as a ‘‘Fowler plot’’ and by a fit of the data to the universal curve one extracts the work function ϕ_0 .

Figure 3 shows a Fowler plot for some of our data on alkali nanoparticles. The temperature is set to that of the heat tube. By varying ϕ_0 to optimize the fit we obtain the temperature-dependent ionization potentials and the estimated accuracy of the fitted value.

Before presenting the results, we would like to address the question of whether the shape of the yield curve may become seriously distorted by the wide particle size distribution in the beam. We made a calculation for a log-normal size distribution (considered to be a typical case for condensation beams³⁰) with an average size of 3–5 nm and a width of ~ 2 nm, as in the aforementioned TOF mass spectrum. The total photoelectron yield was calculated by convoluting the size distribution with a size-dependent photoabsorption cross section and a yield function. For the latter, we used Eq. (1) with a size-dependent ionization threshold $\phi(R)$ given by^{31–33}

$$\phi(R) = \phi_0 + \alpha \frac{e^2}{R}, \quad (3)$$

where ϕ_0 is the work function for a bulk surface, R is the radius of the cluster, and α lies in the range of ~ 0.32 – 0.44 .

The photoabsorption cross section was assumed to scale either with the surface area or with the volume of the particle. In both cases it was found that the shape of the photoyield curve in the threshold region was not measurably

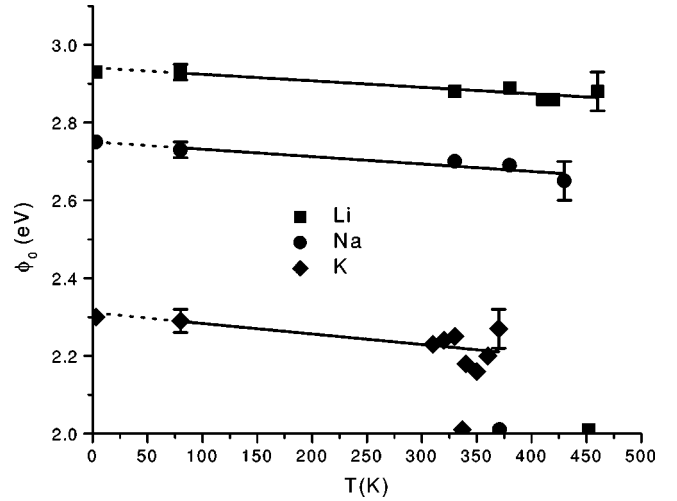


FIG. 4. The experimentally determined work functions as a function of temperature. The solid straight lines are least-squares fits. The dotted lines are extrapolations to the polycrystalline work functions for bulk surfaces at zero temperature (indicated by the points on the y axis) (Ref. 4). The marks on the x axis indicate the bulk melting point for each metal.

altered. Qualitatively, the reason is that all the large particles in the distribution have the same threshold behavior, while the contribution of the smaller ones, shifted away to higher frequencies according to Eq. (3), is suppressed by their smaller cross sections.

IV. RESULTS AND DISCUSSION

The measured temperature-dependent work functions for free nanoparticles of Li, Na, and K are presented in Fig. 4. The lines are a linear least-squares fit. Note that the work functions extrapolate precisely to the literature polycrystalline bulk surface work functions at zero temperature.³⁴ (This is the appropriate limit for the present case: the randomly oriented particles will present multiple nanoscale faces to the light beam. Hence, as in the case of polycrystalline bulk surfaces with ‘‘patches,’’³⁵ the data can be described in terms of single effective work functions.) In contrast, in earlier variable-temperature measurements on bulk alkalis,³⁵ the zero-temperature work functions were significantly shifted from the accepted values (possibly due to difficult-to-combat contamination effects¹¹), although the temperature derivatives were of the same order of magnitude as found here. Note also that the weak temperature-induced work functions shifts were resolved quite reliably by the nanoparticle photoyield data. This attests to the fact that the study of free nanoclusters in beams offers a very accurate complement to traditional surface spectroscopy.

The plot also indicates the position of the bulk melting point for each metal. Within the accuracy of this measurement, no drastic changes were observed in either the work function or the shape of the photoyield curve upon crossing the bulk melting temperature. This is in agreement with the bulk alkali data of Ref. 35.

Figure 5 shows the slopes of the measured $\phi_0(T)$ lines

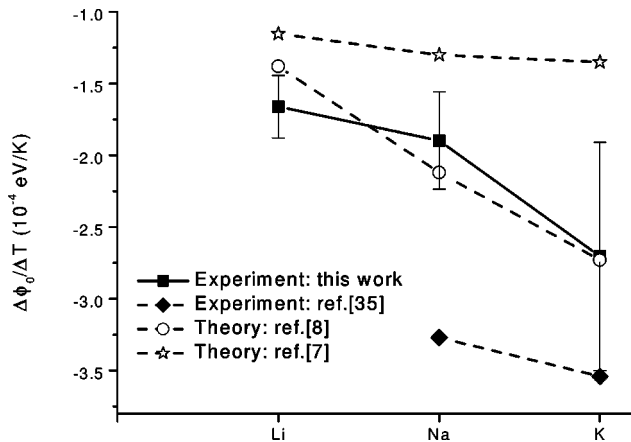


FIG. 5. The slopes of the temperature variation of the work function over the measured interval compared with the calculations of Durakiewicz *et al.* (Ref. 8), Kiejna *et al.* (Ref. 7), and the experiment of Alchagirov *et al.* (Ref. 35).

from Fig. 4 together with the results of an earlier measurement by Alchagirov *et al.*³⁵ Also shown are the calculated $\Delta\phi/\Delta T$ values of Durakiewicz *et al.*⁸ and of Kiejna *et al.*⁷ for the same temperature range.³⁶

The calculation by Durakiewicz *et al.*⁸ is based on the image-charge approximation: the work function is represented as the amount of work needed to remove an electron from a distance d outside the planar surface, where $d \sim$ screening length. The temperature dependence of the work

function here arises primarily from thermal expansion of the metal which results in a decrease of the electron density and a concomitant change of the Fermi energy. While the theory is partly phenomenological, it provides a good fit for most metallic elements^{37,38} and evidently identifies the main scaling variables as far as the temperature dependence of the work function is concerned. Other theories incorporating thermal expansion effects^{7,9,10} predict similar (slightly lower) $\Delta\phi/\Delta T$ slopes.

In summary, we have shown that photoionization spectroscopy of alkali nanoparticles in a beam provides high-accuracy data for the metallic work function and its temperature dependence. The results provide motivation for studies of the influence of temperature on the photoionization spectra of smaller clusters, where thermal expansion has been predicted to have a stronger effect than in the bulk,^{39,40} and of particles composed of materials which exhibit measurable changes in the work function and photoyield at the melting point (e.g., Sn, In, Ga, etc.^{35,41}). Since in smaller clusters the temperature of the melting transition undergoes strong shifts as a function of size,⁴² it is interesting whether photoelectron yield spectra would behave analogously.

ACKNOWLEDGMENTS

We would like to thank V. Kasperovich for his contributions to the experiments, K. Bowen for advice on particle source construction, and C. Wittig for the loan of equipment. This work was supported by the U.S. National Science Foundation under Grant No. PHY-0098533.

*Current address: Chemistry Division, Argonne National Laboratory, Argonne, IL 60439.

¹C. Kittel, *Introduction to Solid State Physics*, 7th ed. (Wiley, New York, 1996).

²A. Zangwill, *Physics at Surfaces* (Cambridge University Press, Cambridge, England, 1988).

³*CRC Handbook of Chemistry and Physics*, 82nd ed., edited by D. R. Lide (CRC Press, London, 2001).

⁴H. B. Michaelson, *J. Appl. Phys.* **48**, 4729 (1977).

⁵C. Herring and M. H. Nichols, *Rev. Mod. Phys.* **21**, 185 (1949).

⁶M. Cardona and L. Ley, in *Photoemission in Solids*, edited by M. Cardona and L. Ley (Springer, Berlin, 1978).

⁷A. Kiejna, K. F. Wojciechowski, and J. Zebrowski, *J. Phys. F: Met. Phys.* **9**, 1361 (1979).

⁸T. Durakiewicz, A. J. Arko, J. J. Joyce, D. P. Moore, and S. Halas, *Surf. Sci.* **478**, 72 (2001).

⁹A. Kiejna, *Surf. Sci.* **178**, 349 (1986).

¹⁰A. Kiejna and V. V. Pogosov, *J. Phys.: Condens. Matter* **8**, 4245 (1996).

¹¹R. J. Whitefield and J. J. Brady, *Phys. Rev. Lett.* **26**, 380 (1971).

¹²H. Burtscher and H. C. Siegmund, in *Clusters of Atoms and Molecules*, edited by H. Haberland (Springer, Berlin, 1994), Vol. II, and references therein.

¹³H. Göhlich, T. Lange, T. Bergmann, U. Näher, and T. P. Martin, *Chem. Phys. Lett.* **187**, 67 (1991).

¹⁴K. Wong, V. Kasperovich, G. Tikhonov, and V. V. Kresin, *Appl. Phys. B: Lasers Opt.* **73**, 407 (2001).

¹⁵P. Milani and S. Iannotta, *Cluster Beam Synthesis of Nanostructured Materials* (Springer, Berlin, 1999).

¹⁶C. Ellert, M. Schmidt, C. Schmitt, T. Reiners, and H. Haberland, *Phys. Rev. Lett.* **75**, 1731 (1995).

¹⁷F. Chandezon, P. M. Hansen, C. Ristori, J. Pedersen, J. Westergaard, and S. Björnholm, *Chem. Phys. Lett.* **277**, 450 (1997).

¹⁸Pulsed laser ionization of large metal clusters generates a significant amount of fragmentation (Refs. 19 and 20). Accordingly, our measured TOF spectra are dominated by fragment peaks, as verified by varying the laser fluence: with decreasing laser pulse power the lower part of the size distribution was found to decrease, while the upper part remained unaffected apart from the overall decrease of the counting rate.

¹⁹C. Bréchnignac, Ph. Cahuzac, F. Carlier, M. de Frutos, and J. Ph. Roux, *Phys. Rev. B* **47**, 2271 (1993).

²⁰W. Bouwen, F. Vanhoutte, F. Despa, S. Bouckaert, S. Neukermans, L. T. Kuhn, H. Weidele, P. Lievens, and R. E. Silverans, *Chem. Phys. Lett.* **314**, 227 (1999).

²¹V. Kasperovich, K. Wong, G. Tikhonov, and V. V. Kresin, *Phys. Rev. Lett.* **85**, 2729 (2000).

²²W. A. Saunders, K. Clemenger, W. A. de Heer, and W. D. Knight, *Phys. Rev. B* **32**, 1366 (1985).

²³W. A. de Heer, W. D. Knight, M. Y. Chou, and M. L. Cohen, in *Solid State Physics*, edited by H. Ehrenreich and D. Turnbull (Academic, New York, 1987), Vol. 40.

²⁴As a manifestation of both particle size and absorption efficiency, a significant ion counting rate (ca. 1 kHz) could be observed

- upon illumination of the beam by a simple pocket flashlight—not a common occurrence in molecular beam studies.
- ²⁵O. Björneholm, F. Federmann, F. Fössing, and T. Möller, *Phys. Rev. Lett.* **74**, 3017 (1995).
- ²⁶C. Bréchiqnac, Ph. Cahuzac, F. Carlier, M. de Frutos, J. Leyqnier, J. Ph. Roux, and A. Sarfati, *J. Phys. II* **2**, 971 (1992).
- ²⁷A. Schmidt-Ott, P. Schurtenberger, and H. C. Siegmann, *Phys. Rev. Lett.* **45**, 1284 (1980).
- ²⁸R. H. Fowler, *Phys. Rev.* **38**, 45 (1931).
- ²⁹U. Müller, H. Burtscher, and A. Schmidt-Ott, *Phys. Rev. B* **38**, 7814 (1988).
- ³⁰C.-R. Wang, R.-B. Huang, Z.-Y. Liu, and L.-S. Zheng, *Chem. Phys. Lett.* **227**, 103 (1994).
- ³¹M. Seidi, K.-H. Meiwes-Broer, and M. Brack, *J. Chem. Phys.* **95**, 1295 (1991).
- ³²W. A. de Heer, *Rev. Mod. Phys.* **65**, 611 (1993).
- ³³C. Bréchiqnac, in *Clusters of Atoms and Molecules*, edited by H. Haberland (Springer, Berlin, 1994), Vol. I.
- ³⁴Our extrapolated zero-temperature work functions show a systematic shift on the order of 0.01 eV above the literature values. According to Eq. (3), a cluster with a radius of 5 nm should have an ionization potential ~ 0.1 eV higher than the work function for a bulk surface. Note, however, that our beam contains a broad distribution of particle sizes, and therefore the yield threshold is dominated by the largest clusters in the distribution, as discussed in Sec. III. Particle sizes from the high end of the TOF mass spectrum bring the size correction term within the overall error bars ($\sim \pm 0.05$ eV) of the extrapolation.
- ³⁵B. B. Alchagirov, K. B. Khokonov, and Z. K. Arkhestov, *Dokl. Phys. Chem.* **326**, 475 (1992) [*Dokl. Akad. Nauk* **326**, 121 (1992)].
- ³⁶To be more precise, Ref. 8 calculates the work function as a quadratic, rather than linear, function of temperature. However, within the range and accuracy of our data a linear fit is adequate.
- ³⁷S. Halas and T. Durakiewicz, *J. Phys.: Condens. Matter* **10**, 10815 (1998).
- ³⁸T. Durakiewicz, S. Halas, A. Arko, J. J. Joyce, and D. P. Moore, *Phys. Rev. B* **64**, 045 101 (2001).
- ³⁹N. Ju and A. Bulgac, *Phys. Rev. B* **48**, 2721 (1993).
- ⁴⁰S. Kümmel, J. Akola, and M. Manninen, *Phys. Rev. Lett.* **84**, 3827 (2000).
- ⁴¹P. Oelhafen and U. Gubler, in *Electrons in Disordered Metals and at Metallic Surfaces*, edited by P. Phariseau, B. L. Györfy, and L. Scheire (Plenum, New York, 1979).
- ⁴²M. Schmidt, R. Kusche, B. von Issendorff, and H. Haberland, *Nature (London)* **393**, 238 (1998).